14th European Conference on Mixing
Warszawa, 10-13 September 2012

MIXING AND RECIRCULATION CHARACTERISTICS OF GAS-LIQUID TAYLOR FLOW IN MICROREACTORS

T. Abadie[a,b], J. Aubin[a], C. Xuereb[a], D. Legendre[b].

[a] *University of Toulouse, Laboratoire de Génie Chimique CNRS/INPT/UPS, 4 Allée Emile Monso, BP-84234, 31030 Toulouse, France;*

[b] *University of Toulouse, Institut de Mécanique des Fluides CNRS/INPT/UPS, 1 Allée du Prof. Camille Soula, 31400 Toulouse, France*
joelle.aubincano@ensiacet.fr

Abstract. The effects of operating parameters (capillary and Reynolds numbers) and microchannel aspect ratio ($\alpha = w/h = [1, 2.5, 4]$) on the recirculation characteristics of the liquid slug in gas-liquid Taylor flow in microchannels has been investigated using 3-dimensional Volume Of Fluid numerical simulations. The results show good agreement with previous results in circular and square geometries [20] with a decrease in the recirculating volume in the slug and an increase in recirculation time with increasing capillary number. In addition, increasing the aspect ratio of the channel leads to a slight decrease in recirculating volumes and a significant increase in recirculation times.

Keywords: gas-liquid Taylor flow, microchannel, microreactor, mixing, recirculation, CFD, VOF.

1. INTRODUCTION

Over the last decade, micro reaction technology has become of much interest to both academics and the process industries for the intensification of chemical processes. Taylor or slug flow is a commonly encountered flow regime for gas-liquid microchannel flows and has the advantage of providing high interfacial area and good liquid mixing in the liquid slug, thereby enhancing transport processes. These features of microreactors are particularly interesting for fast and highly exothermic gas-liquid reactions – amongst other applications – and allow an increase in reaction performance whilst working under safe operating conditions ([10],[12]). A number of studies have focused on the understanding of hydrodynamics, as well as the heat and mass transfer enhancement in these flows (see reviews [14],[18],[9]) but often independently. Indeed the transport efficiency appears to be closely related to the recirculation in the liquid phase, which depends on the operating conditions, fluid properties and reactor geometry.

A major feature of gas-liquid Taylor flow is the recirculation flow pattern generated in the liquid slug in the moving frame of reference as shown in Fig. 1 and detailed in [19]. The flow pattern is characterized by the position of the centre of the circulation loop [x_0, y_0], and the position of the streamline separating the recirculation zone and the liquid film at the channel wall [x_1, y_1]. As the bubble velocity increases, both the loop centre and the outer streamline of the recirculation zone move towards the centre of the channel (see [20] for circular and square capillaries). This leads to a reduction of the volume of the recirculating zone and an increase in the volume of liquid in the film region until complete bypass flow occurs at $U_B \geq U_{max}$. Little information, however, on the characteristics of the recirculation zone in rectangular channels is available but a common observation is that a key parameter to characterize the recirculation and film zones is the dimensionless velocity $W = (U_B - U_{TP}) / U_B$ where U_B is the bubble velocity and U_{TP} the mean velocity in the slug. Recently, it has been shown theoretically [13] that the cross-sectional area occupied by the recirculation zone

is generally smaller for rectangular channels compared with circular channels due to the increased film thickness in the channel corners causing a decrease in the recirculation time.

The recirculation time in the liquid slug in Taylor flow is defined as the time required for an element of fluid to complete one revolution in the recirculating slug. This characteristic time is particularly relevant for transport processes occurring in the system, such as mass transfer between the bubble and slug or wall and slug, and heat transfer with the channel wall. The rate of flow recirculation is calculated via the surface integration of the relative velocity profile across the microchannel cross-section, similarly to what is done in conventional stirred tanks to calculate circulation induced by the mechanical impeller [11]. The recirculation flow rate through the microchannel can be divided into three parts:

- a positive flow rate, Q_0, in the main flow direction at central core of the microchannel occupying a volume V_0 with a cross-sectional area A_0,
- a negative flow rate, Q_1, with a volume V_1 and a cross-sectional area A_1 that corresponds to the recirculating liquid in the slug,
- a negative flow rate, Q_2 of volume V_2 in area A_2, close to the channel wall, which contributes to axial mixing between slugs instead of radial mixing within the slug.

The recirculation time is then defined as $t_{rc} = V_{rc} / Q_{rc}$, where the recirculating volume V_{rc} corresponds to the volume of liquid within the limit of the separating streamline and Q_{rc} is the recirculation flow rate equal to Q_0 (and $|Q_1|$). t_{rc} is made non dimensional : $\tau_{rc} = t_{rc} / (L_S/U_B)$.

In our previous work we have explored the effects of fluid properties, operating conditions and microchannel geometry on Taylor bubble size [1] and the flow patterns in the liquid slug using micro Particle Image Velocimetry (μ-PIV) [22]. The objective of this work is to explore the effects of operating parameters (capillary, *Ca*, and Reynolds numbers, *Re*) and microchannel aspect ratio ($\alpha = w/h = [1, 2.5, 4]$) on the mixing and recirculation characteristics of the liquid slug in gas-liquid Taylor flow in microchannels. To do this, 3-dimensional VOF simulations of gas-liquid Taylor flow in microchannels have been performed. Using an approach which is analogous to the determination of circulation rate in stirred tanks, the recirculation rate in the liquid slug, as well as the size of the recirculating zone have been evaluated from the numerical data. An attempt has been made to relate these characteristics of the recirculating liquid slug to the enhanced transport phenomena observed in such systems. Finally, recommendations on the design and operation of microreactors employing Taylor flow are given.

2. METHODOLOGY

2.1 Theoretical developed velocity profile in rectangular capillaries

The theoretical velocity profile in a cross section of a rectangular capillary has been used to evaluate the effects of aspect ratio and dimensionless bubble velocity on characteristic parameters of recirculation motion in gas-liquid Taylor flow: recirculating volumes and recirculation times. Under the assumption that the slug is long when compared with development lengths of velocity profile at the rear and the nose caps of the bubbles, the recirculation volume and its cross section area are proportional since $V_{0,1} = A_{0,1} L_S$.

The velocity profile in a rectangular capillary with a cross section $2w \times 2h$ is :

$$u(x,y) = -\frac{16 c_1 w^2}{\pi^3} \sum_{n=1,3,\dots}^{+\infty} \frac{(-1)^{\frac{(n-1)}{2}}}{n^3} \left[1 - \frac{\cosh\left(\frac{n\pi y}{2w}\right)}{\cosh\left(\frac{n\pi h}{2w}\right)}\right] \cos\left(\frac{n\pi x}{2w}\right)$$

$$U_{TP} = -\frac{c_1 w^2}{3} \left[1 - \frac{192}{\pi^5}\frac{w}{h} \sum_{n=1,3,\dots}^{+\infty} \frac{1}{n^5} \tanh\left(\frac{n\pi h}{2w}\right)\right]$$

where w is the channel width, h is the height and c_1 is a constant for a given value of U_{TP}. Integration of these profiles allows the prediction of recirculating volumes and recirculation times as a function of the aspect ratio and the dimensionless velocity W in the case of long slugs.

2.2 Numerical simulations

The numerical code used for this study is the JADIM code ([1],[3],[6],[16],[17]) to perform direct numerical simulations of two-phase flows. The interface capturing technique implemented in this code is the Volume Of Fluid method (VOF) which consists in a Eulerian description of each phase on a fixed grid introducing a volume fraction of each phase in every cell. The interface location and thickness are both controlled by an accurate algorithm based on Flux-Corrected Transport schemes [20] and the Continuum Surface Force (CSF) [4] is used to calculate the surface tension source term in the momentum equation.

Since the effects due to gravity in microchannels can be neglected (*Bo ~ gravity/(surface tension) < 0.1*), only a quarter of the channel is considered. The bubble is placed in the domain and a pressure gradient between two periodic boundary conditions is imposed to induce the motion until the flow reaches a steady state. No-slip wall conditions are imposed on the planes $x = w$ and $y = h$ while symmetry boundary condition is set at $x = 0$ and $y = 0$. The grids used consist of 32x32x256, 48x32x256 and 64x32x256 cells for microchannels with aspect ratios of 1, 2.5 and 4, respectively. These grids are refined at the walls in order to correctly resolve the thin liquid film between the bubble and the wall.

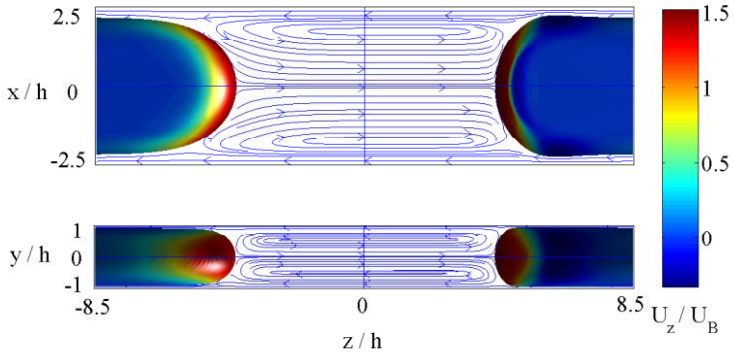

Fig. 1: Illustration of the bubble shape and the streamlines in the cross sections of a rectangular capillary with an aspect ratio of *2.5* (top and side views). The axial velocity on the bubble interface is shown ($U_z(x,y,z) / U_B$). *Ca ~ 0.05* and *Re ~ 14*.

3. RESULTS & DISCUSSION

3.1. Centre and size of the recirculation zone

Recirculation areas approximated from the theoretical fully developed velocity profile have been calculated and are shown in Fig. 2 for 3 geometries : *w/h = [1, 2.5, 4]*. It can be seen that the recirculation areas follow the shape of the channel for low dimensionless velocities and tend to circular and elliptical shapes depending on the aspect ratio while moving towards the center of the channel at the same time.

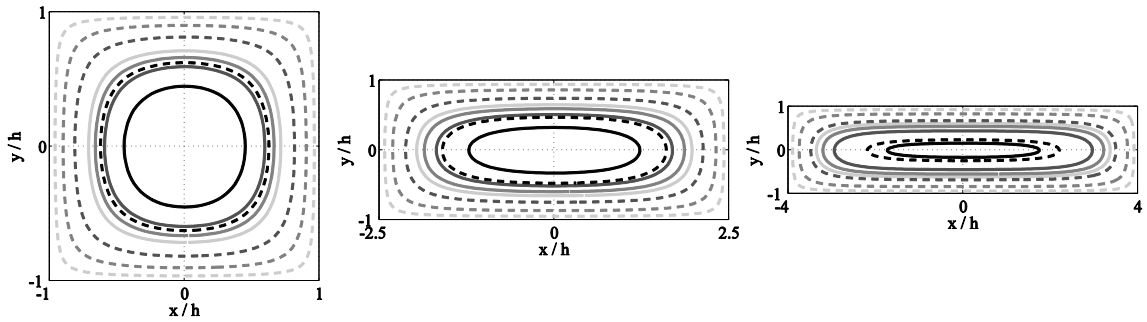

Fig. 2 : Cross section of the recirculation loops for aspect ratios *w/h = [1, 2.5, 4]*. Legend : (—) center of the recirculation loop ; (---) streamline separating the circulation loop and the film. From the walls to the center (light gray to black) : *W = [0.1 ; 0.2 ; 0.3 ; 0.42]*.

When the channel aspect ratio increases, the aspect ratio of the recirculation zone also increases. Furthermore, the center of the recirculation loop and the separating streamline both

move faster towards the center of the channel in the less confined direction. As a result, the slug film thickness is greater in the width of the microchannel than in the height.

3.2. Characteristic recirculating volumes

A characteristic parameter of the recirculation motion in Taylor flow is the volume of fluid recirculating in the slug. Unlike in cylindrical tubes where the volumes of positive flow and negative flow of the recirculation region are equal, it is not the case in square and rectangular ducts. Indeed, in the channel cross-section the ratio of total recirculation area over positive recirculation area is a function of the aspect ratio and tends to $\sqrt{3}$ for the asymptotic behavior of an infinite aspect ratio. In addition, for a fixed geometry, the ratio of recirculation areas also varies with the dimensionless velocity *W*.

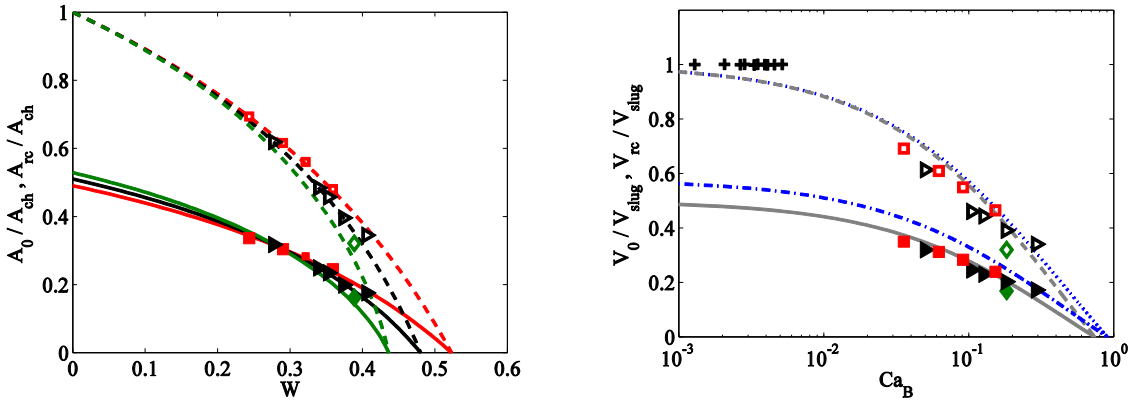

(a) (b)

Fig. 3: (a) Dimensionless cross section of the recirculating areas at the centre of the slug versus the dimensionless bubble velocity. Legend : (—) A_0/A_{ch}; (---) A_{rc}/A_{ch}; (□, red) *w/h = 1*; (▷, black) *w/h = 2.5*; (◊, green) *w/h = 4*. (b) Dimensionless recirculating volumes versus capillary number. Legend : (—, gray) V_0/V_{slug} axi; (---, gray) V_{rc}/V_{slug} axi; (-•-, blue) V_0/V_{slug} 2D; (•••, blue) V_{rc}/V_{slug} 2D; (□, red) *w/h = 1*; (▷, black) *w/h = 2.5*; (◊, green) *w/h = 4*; (+, black) V_{rc}/V_{slug} exp, *w/ h =2.5*.

The calculations of the recirculation areas and volumes at the center of the slugs for aspect ratios *[1, 2.5, 4]* are shown in Fig. 3(a). Very good agreement between the computational and theoretical results is observed, as long as the liquid velocity profile is fully developed at the center of the slug. The two computations that show a slight deviation from the theory correspond to cases where the velocity profile is not entirely fully developed.

For short slugs where the laminar velocity profile is not fully developed and the region where the flow is disturbed by the bubble is not negligible, the recirculating volumes and times can therefore not be approximated by the theoretical velocity profile. In such cases, the recirculating volume is obtained from direct numerical simulations by integrating small slices of recirculating zones along the slug. The volume of liquid recirculating around the bubble between the bubble body and its caps is deliberately not considered here since bubble to liquid mass transfer in this region is assumed to be by the diffusional mechanism only.

Fig. 3(b) shows the ratio of recirculating volumes over total slug volume as a function of the capillary number for three rectangular geometries. The recirculating volumes for the infinite aspect ratio and axisymetrical cases are also given using the relation *W = f(Ca)* from [2] for the tubes and [1] for 2D cases and with the assumption of a long slug in order to neglect the changes in the flow close to the bubble caps. Experimental data obtained by µ-PIV [22] are also presented. As expected, the recirculating volumes are close to the slug volume at low capillary numbers ($Ca_B \sim 10^{-3}$) due to the fact that the bypass flow is negligible compared with the total flow rate. In other words, almost all the liquid contributes to the recirculation motion. Then, when the capillary number increases, the recirculating volume decreases in all the geometries. While the volume of the positive recirculating flow is hardly dependent on the geometry, the total recirculating volume decreases as the aspect ratio increases.

For a given dimensionless velocity, the flow rate in the bypass film is constant. However, the cross sectional area occupied by the bypass flow increases with the channel aspect ratio and therefore the mean velocity in the slug film decreases when the aspect ratio increases. As a consequence, for a given dimensionless velocity, the axial dispersion will be more limited in geometries with high aspect ratio.

3.3. Characteristic recirculation times

The characteristic recirculation times – τ_0 for the positive recirculation flow, τ_1 for the negative flow and τ_{rc} for the total recirculation –as a function of the dimensionless velocity and the capillary number are plotted in Fig. 4(a) and (b), respectively.

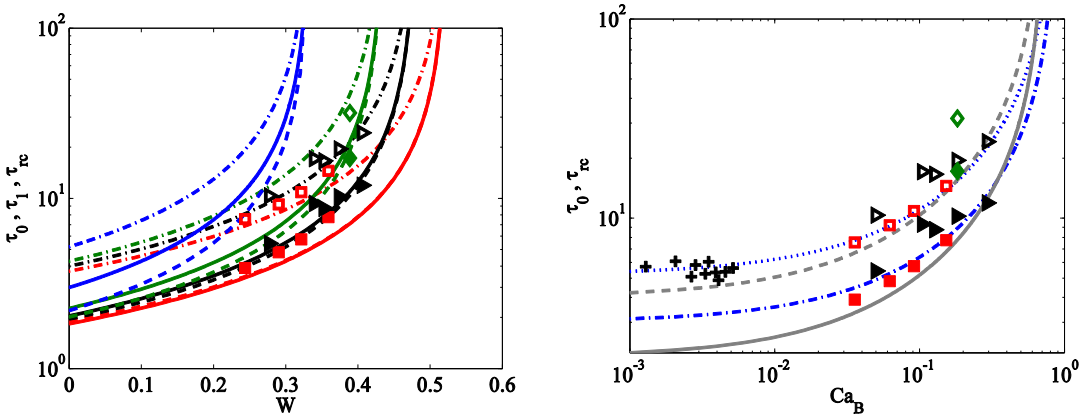

Fig. 4: (a) Dimensionless recirculation times versus the dimensionless bubble velocity. Legend : (—) τ_0; (---) τ_1 ; (-•-) τ_{rc} ; (□, red) *w/h = 1*; (, black) *w/h = 2.5*; (◊, green) *w/h = 4*; (blue) 2D. (b) Dimensionless recirculation times versus capillary number. Legend : (—, gray) τ_0 axi; (---, gray) τ_{rc} axi; (-•-, blue) τ_0 2D; (•••, blue) τ_{rc} 2D; (filled symbols) τ_0; (empty symbols) τ_{rc}; (□, red) *w/h = 1*; (▷, black) *w/h = 2.5*; (◊, green) *w/h = 4*; (+, black) τ_{rc} exp, *w/ h =2.5*.

Although the recirculation areas show good agreement with the theoretical predictions, the recirculation times τ_{rc} are greater than those determined using the infinite slug assumption (Fig. 4(a)). Indeed, close to bubble caps where the flow is disturbed, the axial flow rate is reduced and the real recirculation time is increased. The trends observed for all geometries are qualitatively similar and increasing the aspect ratio leads to an increase in both positive and negative recirculation times and thus on the total recirculation time.

Fig. 4(b) shows that an increase in the capillary number also leads to an increase in the recirculation time for all the geometries. This is the opposite trend observed for the recirculation volume in Fig. 3(b). It is also observed that the 2D theory is not a good approximation for high aspect ratios. In addition, it can be seen that even if the recirculating volumes showed a weak dependency on the geometry, the differences observed on the recirculation times are more significant and radial mixing is reduced when increasing the aspect ratio at fixed operating conditions (*Ca*, *Re* and L_S) .

4. CONCLUSION

Numerical simulations have been compared with theoretical approximations for the case of infinite slugs in terms of cross-sectional recirculation areas, recirculating volumes and recirculation times. It has been shown that as long as the slug is long, the recirculation area in the slug can be well predicted using the fully developed velocity profile. Whatever the geometry, increasing the capillary number leads to a decrease in recirculating volume and an increase in recirculation time, which means that transport processes will be hindered. Radial mixing is then reduced while axial dispersion is enhanced with increasing the capillary number. It has been shown that for a given capillary number, when the aspect ratio increases the recirculating volume decreases slightly, however the recirculation time increases. Indeed,

high aspect ratio channel may appear attractive for heat transfer in plate microreactors, however this decrease in the recirculation rate and effective recirculation volume is disadvantageous for both heat and mass transfer operations. It is therefore expected that some intermediate aspect ratio geometry would be most effective. The disturbed flow close to the bubble caps has shown to generally increase recirculation time and it is expected that as the slug length increases, the recirculation time tends to that predicted by the fully developed velocity profile. A comprehensive study of the effects of operating conditions and geometry on development length in the slug ahead and in the wake of a Taylor bubble will be carried on to thoroughly characterize the role of the slug length on the recirculation parameters.

ACKNOWLEDGEMENTS

This work was financed by the French "Agence Nationale de la Recherche" in the framework of the project MIGALI no. ANR-09-BLAN-0381-01. We also acknowledge the support for this project from the CNRS research federation FERMaT, such as the CALMIP project for providing computational resources.

5. REFERENCES

[1] T. Abadie, J. Aubin, D. Legendre, C. Xuereb, 2011. "Hydrodynamics of gas-liquid Taylor flow in rectangular microchannels", *Microfluid Nanofluid*, DOI 10.1007/s10404-011-0880-8.
[2] P. Aussillous, D. Quere, 2000. "Quick deposition of a fluid on the wall of a tube", *Phys. Fluids*, **12**(10):2367
[3] T. Bonometti, J. Magnaudet, 2007. "An interface-capturing method for incompressible two-phase flows. Validation and application to bubble dynamics", *Int. J. Multiph. Flow*, **33**, 109-133.
[4] J. Brackbill, D.B. Kothe, C. Zemach, 1992. "A continuum method for modeling surface tension", *J. Comput. Phys.*, **100**, 335-354.
[5] F.P. Bretherton, 1961. "The motion of long bubbles in tubes", *J. Fluid Mech.*, **10**, 166.
[6] J-B. Dupont, D. Legendre, 2010. "Numerical simulation of static and sliding drop with contact angle hysteresis", *J. Comput. Phys.*, **229**, 2453-2478.
[7] R. Gupta, D.F. Fletcher, B.S. Haynes, 2009. "On the CFD modelling of Taylor flow in microchannels", *Chem. Eng. Sci.*, **64**, 2941-2950.
[8] R. Gupta, D.F. Fletcher, B.S. Haynes, 2010. "CFD modelling of heat and mass transfer in the Taylor flow regime", *Chem. Eng. Sci.*, **65**, 2094-2107.
[9] R. Gupta, D.F. Fletcher, B.S. Haynes, 2010. "Taylor flow in microchannels: a review of experimental and computational work", *J. Comp. Multi. Flows*, **2**, 1.
[10] V. Hessel, P. Angelli, A. Gavriilidis, H. Lowe, 2005. "Gas-liquid and gas-liquid-solid microstructured reactors: contacting principles and applications", *Ind. Eng. Chem. Res.*, **44**, 9750.
[11] Jaworski, Z., Nienow, A.W., Dyster, K.N., 1996. "An LDA study of the turbulent flow field in a baffled vessel agitated by an axial, down-pumping hydrofoil impeller", *Can. J. Chem. Eng.*, **74**, 3-15.
[12] M.H. Kashid, L. Kiwi-Minsker, 2009. "Microstructured Reactors for Multiphase Reactions: State of the Art", *Ind. Eng. Chem. Res.*, **48**, 6465-6485.
[13] S. Kececi, M. Worner, A. Onea, H S. Soyhan, 2009. "Recirculation time and liquid slug mass transfer in co-current upward and downward Taylor flow", *Catalysis Today*, **147S**, S125-S131
[14] M.T. Kreutzer, F. Kapteijn, J.A. Moulijn, J.J. Heiszwolf, 2005. "Multiphase monolith reactors: chemical reaction engineering of segmented flows in microchannels", *Chem. Eng. Sci*., **60**, 5895-5916.
[15] D. Liu, S. Wang, 2008. "Hydrodynamics of Taylor flow in noncircular capillaries", *Chem. Eng. Process.*, **47**, 2098-2106.
[16] F. Sarrazin, T. Bonometti, K. Loubiere, L. Prat, C. Gourdon, J. Magnaudet, 2006. "Experimental and numerical study of droplets hydrodynamics in microchannels", *AIChE J.*, **52**, 4061-4070.
[17] F. Sarrazin, T. Bonometti, K. Loubiere, L. Prat, C. Gourdon, J. Magnaudet, 2006. "Hydrodynamic structures of droplets engineered in rectangular microchannels", *Microfluid Nanofluid*, DOI 10.1007/s10404-007-0233-9.
[18] N. Shao, A. Gavriilidis, P., Angeli, 2009. "Flow regimes for adiabatic gas-liquid flow in microchannels", *Chem. Eng. Sci.*, **64**, 2749-2761.
[19] GI. Taylor, 1961. "Deposition of a viscous fluid on the wall of a tube", J Fluid Mech, 10:161-165
[20] Thulasidas, T. C., Abraham, M. A., Cerro, R. L., 1997. "Flow patterns in liquid slugs during bubble-train flow inside capillaries". *Chem. Eng. Sci.*, **52**, 2947-2962.
[21] S.T. Zalesak, 1979. "Fully multidimensional flux-corrected transport algorithms for fluids", *J. Comput. Phys.*, **31**, 335-362.
[22] P. Zaloha, J. Kristal, V. Jiricny, N. Volkel, C. Xuereb, J. Aubin, 2012. "Characteristics of liquid slugs in gas-liquid Taylor flow in microchannels", *Chem. Eng. Sci.*, **68**, 640-649.